Turbulent superfluid profiles in a counterflow channel

L. Galantucci[a,b], C. F. Barenghi[b], M. Sciacca[b,c], M. Quadrio[a] and P. Luchini[d]

[a] Dip. Ingegneria Aerospaziale, Politecnico di Milano, Italia; [b] School of Mathematics and Statistics, Newcastle University, UK;
[c] Dip. Metodi e Modelli Matematici, Università di Palermo, Italia; [d] Dip. Meccanica, Università di Salerno, Italia

Introduction

The recent development of visualization techniques in superfluid helium based on micron-size tracers [1, 2] and laser-induced-fluorescence of metastable helium molecules [3] has raised the possibility of experimentally determining superfluid and normal fluid profiles and the spatial distribution of quantised vortices in a channel.

In this work we are in particular interested in the turbulent flow induced in a plane channel by heat transfer (counterflow turbulence). It is well known that if the applied heat flux $\dot{Q}$ is less than a small critical value $\dot{Q}_c$ then the heat is carried by the laminar Poiseuille flow of normal fluid component, and the vortex–free superfluid component flows uniformly in the opposite direction to conserve mass. If $\dot{Q} > \dot{Q}_c$ the superfluid component becomes turbulent, forming a disorganized tangle of quantised vortices, while the normal fluid might still be laminar or undergo a transition leading to a turbulent state (Tough 1982, Melotte & Barenghi 1998).

We are concentrated on the intermediate heat transfer regime, in which the normal fluid is still laminar, while the superfluid forms a turbulent tangle. Within this flow pattern, we consider three different vortex re-nucleation regimes in order to conserve the vortex–line density and therefore maintain a steady state.

The aim of this work [4] is to determine for the different nucleation regimes considered the average steady–state superfluid velocity profile $\mathbf{v}_s(y)$ and the average spatial distribution of the vortices $n(y)$ at scales larger than the average vortex separation ℓ but smaller than the channel size D.

Model

We calculate the temporal evolution of N vortex–points positions in an idealised two-dimensional plane channel with walls at $y = \pm D/2$ and periodic boundary conditions at $x = 0$ and $x = \lambda$.

Half the N vortices have positive circulation $\Gamma_j = \kappa$ and half negative circulation $\Gamma_j = -\kappa$, where $\kappa = 10^{-3}\ \mathrm{cm}^2/\mathrm{s}$ is the quantum of circulation in superfluid ^{4}He. The equation of motion of a vortex located at $\mathbf{r}_j$ is (Schwarz 1988),

$$\begin{aligned}\frac{d\mathbf{r}_j}{dt} = & \ \mathbf{v}_{s0}(t) + \mathbf{v}_{si}(\mathbf{r}_j, t) \\ & + \ \alpha \mathbf{s}'(\mathbf{r}_j) \times (\mathbf{v}_n(\mathbf{r}_j) - \mathbf{v}_{s0}(t) - \mathbf{v}_{si}(\mathbf{r}_j, t)) \\ & + \ \alpha'(\mathbf{v}_n(\mathbf{r}_j) - \mathbf{v}_{s0}(t) - \mathbf{v}_{si}(\mathbf{r}_j, t)),\end{aligned}$$

where: $\mathbf{s}'_j$ is the unit vector along the vortex j; α and α' are mutual friction coefficients; $\mathbf{v}_n = -V_{n0}[1 - (2y/D)^2]\hat{\mathbf{x}}$, $V_{n0} > 0$ is the normal fluid profile which we assume to be a Poiseuille classical profile; $\mathbf{v}_{si}$ is the induced superfluid velocity field created by the vortices in $\mathbf{r}_j$; $\mathbf{v}_{s0} = V_{s0}(t)\hat{\mathbf{x}}$, $V_{s0}(t) > 0$ is the uniform superfluid flow which enforces the counterflow condition of no net mass flow along the channel.

To model the creation and destruction of vortices within our model, when the distance between two vortex–points of opposite circulation becomes smaller than a critical value ϵ_1 or when the distance between a vortex and a boundary is less than $\epsilon_2 = \epsilon_1/2$, we perform a *numerical vortex reconnection* and remove these vortices.

To maintain a steady state, when a vortex is removed a new vortex of the same circulation is re-inserted into the channel following three different *re-nucleation regimes* (in red the corresponding three-dimensional superfluid vorticity production mechanism):

- case (a) : randomly in the channel (superfluid vorticity produced by the vortex tangle)
- case (b) : on the channel axis
- case (c) : near the walls (superfluid vorticity produced by wall-pinned vortices)

Numerical Parameters

The governing equations solved numerically are written in dimensionless form employing the following units of length, velocity and time, respectively $\delta_c = D/2 = 4.55 \times 10^{-3}$ cm , $u_c = \kappa/(2\pi\delta_c) = 3.49 \times 10^{-2}$ cm/s, $t_c = \delta_c/u_c = 0.13$ s. Non-dimensional quantities are denoted by the superscript '$*$'.

We choose the parameters of the simulations taking into account the experiments of Tough *et al.* (1979,1983): $T = 1.7$°K, $D^* = 2$, $\lambda^* = 6$, $N_1 = 1876$ and $N_2 = 4800$. To make connection with experiments, we interpret $n = N/(\lambda D)$ (number of vortex points per unit area) as the vortex line density L (vortex length per unit volume), from which $\ell = n^{-1/2}$ is the average intervortex spacing.

The values N_1 and N_2 lead respectively to $\ell_1^* \approx 0.08$ and $\ell_2^* \approx 0.05$ which correspond to the dimensionless numbers $L_1^{1/2}D = 25$ and $L_2^{1/2}D = 40$ (typical of counterflow experiments). The maximum normal fluid velocities $V_{n0_1}^* = 553.6$ and $V_{n0_2}^* = 882.3$ are consistently determined employing experimental data.

Vortex configurations

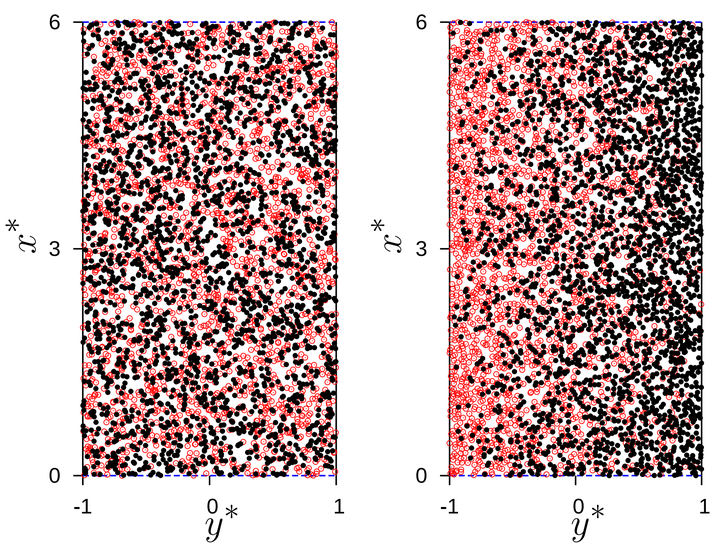

FIGURE 1: Initial random vortex configuration (left) and steady state vortex configuration (right) for case (a) and $N_2 = 4800$. Positive and negative vortices are respectively denoted by empty red and filled black circles.

Fig. 1 compares, for case (a) and $N_2 = 4800$, the steady state vortex configuration reached after a transient interval $\tau_a^* = 1 \times 10^{-2}$ with the initial random configuration shared by all three cases. A strong - but not complete - polarization is seen to characterize the steady state, in agreement with Barenghi *et al.* (2002).

Superfluid Velocity Profiles

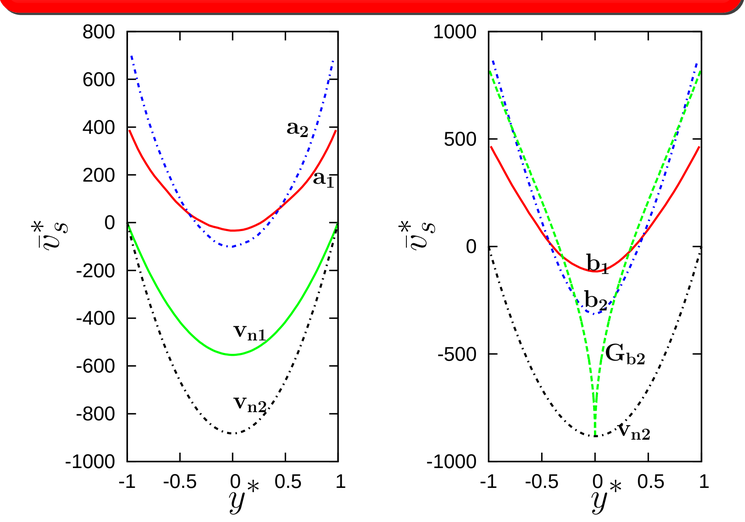

FIGURE 2: Left. Coarse-grained superfluid velocity $\bar{v}_s^*(y^*)$ for case (a): solid red line a_1 for $N = 1876$, dot-dashed blue line a_2 for $N = 4800$. Normal fluid velocity profile for $N = 1876$ (solid green line v_{n1}) and $N = 4800$ (dot-dashed black line v_{n2}). Right. $\bar{v}_s^*(y^*)$ for case (b): solid red line b_1 for $N = 1876$; dot-dashed blue line b_2 for $N = 4800$. Dashed green line G_{b2}: analytical laminar solution of HVBK equations deduced applying Geurst's approach (Geurst,1979) to Cartesian geometry.

Given the vortex configuration $\mathbf{r}_j(t)$ $(j = 1, \cdots N)$ we define a *coarse-grained* superfluid velocity $\bar{\mathbf{v}}_s$ by averaging the components of the (microscopic) velocity $\mathbf{v}_s$ over channel strips of size Δ in the y direction, such that $\ell < \Delta < D$ (the limit $\ell \ll \Delta \ll D$ corresponds to the Hall - Vinen - Bekarevich - Khalatnikov (HVBK) equations).

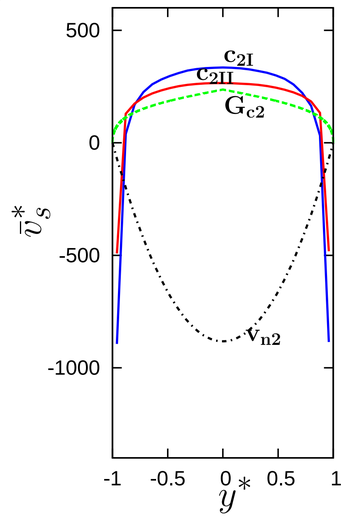

FIGURE 3: Coarse-grained superfluid velocity $\bar{v}_s^*(y^*)$ for case (c) and $N_2 = 4800$. Solid lines c_{2I} (blue) and c_{2II} (red) correspond respectively to nucleation distances from the wall $\xi_1 = \ell$ and $\xi_2 = \ell/2$. Dashed green line G_{c2}: analytical laminar solution of HVBK equations.

Fig. 2 and 3 show the dependence of the profile $\bar{v}_s^*(y^*)$ on N and on the nucleation regimes considered. Note the exactly parabolic profile for case (a_2), the agreement between numerical and analytical solutions in large regions of the channel and the opposite convexity shown by curves (c) and curves (a) and (b).

Vortex Density Profiles

On the same lengthscale Δ we define the average vortex density $n^*(y^*)$ and the average positive vortex density $n_+^*(y^*)$. The corrispondent profiles for $N_2 = 4800$ are plotted in Fig. 4.

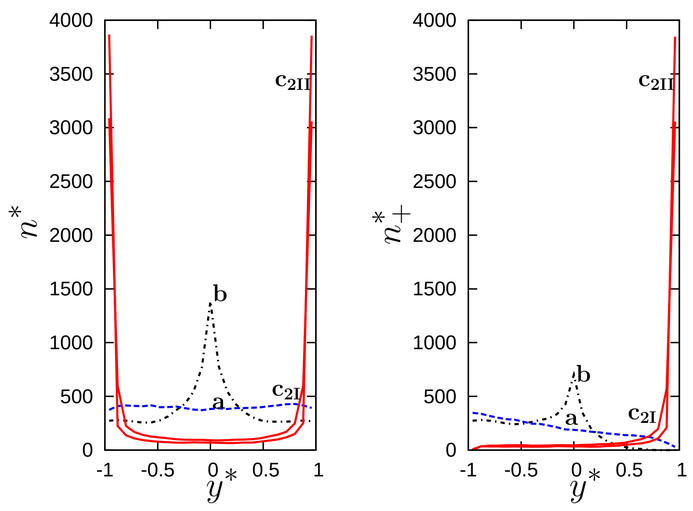

FIGURE 4: Vortex density profiles $n^*(y^*)$ (left) and positive vortex density profiles $n_+^*(y^*)$ (right) for $N_2 = 4800$ and the nucleation regimes considered in this work.

Note the uniform profile of n^* (left) and the partial vortex distribution polarization (right) for case (a), consistently with Fig. 1. An even more intense polarization is observed in case (b).

Conclusions

- Profiles of $\bar{v}_s^*(y^*)$ and $n^*(y^*)$ show a strong dependence on the re-nucleation models adopted; a dependence on N is also clearly observed.
- Comparison of the vortex density profiles n^* in Fig. 4 with experimental results obtained with the technique described in [1] can
  - establish the predominant superfluid vorticity production mechanism
  - predict the coarse-grained superfluid velocity profile $\bar{v}_s^*(y^*)$ in a channel.

References

[1] G.P. Bewley *et al.* , Nature, **441**, 588 (2006).

[2] T. Zhang and S.W. Van Sciver, Nature Physics, **1**, 36 (2005).

[3] W. Guo *et al.* Phys. Rev. Letters **105** 045301 (2010).

[4] L. Galantucci, C. F. Barenghi, M. Sciacca, M. Quadrio and P. Luchini, arXiv:1006.3183v1